Angewandte
Eine Zeitschrift der Gesellschaft Deutscher Chemiker
Chemie

Supporting Information

^{1}H-Detected Solid-State NMR Studies of Water-Inaccessible Proteins In Vitro and In Situ

*João Medeiros-Silva, Deni Mance, Mark Daniëls, Shehrazade Jekhmane, Klaartje Houben, Marc Baldus, and Markus Weingarth**

anie_201606594_sm_miscellaneous_information.pdf

Table of contents:

S1. ^{1}H-linewidth comparison between fully protonated (FP) and inversely fractionally deuterated (iFD) ubiquitin

Note that we prepared and measured two different samples of FP ubiquitin to diminish the influence of the sample quality on the linewidth. Only the FP sample that gave the best linewidth was considered for the evaluation. The ^{15}N linewidth, which is most sensitivity to sample heterogeneity, was virtually exactly the same for the iFD and the FP ubiquitin samples that we compared (Figure S2D), which strongly corroborates that we compared samples of similar quality.

H^N linewidth:

Field	950 MHz	950 MHz	800 MHz	800 MHz	800 MHz	800 MHz	800 MHz
Residue	**iFD [Hz]**	**iFD [ppm]**	**iFD [Hz]**	**iFD [ppm]**	**FP [Hz]**	**FP [ppm]**	**FP/iFD (%)**
T9	127	0.134	138	0.173	147	0.184	6.52
G10	135	0.142	135	0.169	143	0.179	6.06
K11	144	0.152	169	0.212	197	0.246	16.42
I13	188	0.198	193	0.241	219	0.274	13.41
S20	139	0.146	149	0.186	197	0.247	32.50
D21	122	0.128	106	0.133	178	0.223	67.31
K33	141	0.148	136	0.170	171	0.214	26.00
I36	205	0.216	206	0.257	242	0.303	17.93
D39	188	0.198	226	0.282	254	0.318	12.50
Q40	161	0.169	198	0.248	289	0.361	45.74
A46	178	0.187	192	0.240	205	0.256	6.63
G47	119	0.125	119	0.149	116	0.145	-2.36
K48	104	0.109	91	0.114	119	0.148	29.76
Q49	183	0.193	166	0.208	213	0.266	28.04
T55	180	0.189	192	0.239	198	0.248	3.55
Y59	119	0.125	110	0.138	201	0.251	81.65
I61	179	0.188	188	0.235	223	0.279	18.62
S65	87	0.092	84	0.105	155	0.193	84.82
T66	156	0.164	179	0.223	257	0.321	43.98
Average	**150**	**0.158**	**156.67**	**0.196**	**196**	**0.245**	**28.37**

Hα linewidth:

Field	950 MHz	950 MHz	800 MHz	800 MHz	800 MHz	800 MHz	800 MHz
Residue	**iFD [Hz]**	**iFD [ppm]**	**iFD [Hz]**	**iFD [ppm]**	**FP [Hz]**	**FP [ppm]**	**FP/iFD (%)**
L15	135	0.142	140	0.175	230	0.287	**64.23**
V17	103	0.108	115	0.143	152	0.190	**32.25**
P19	200	0.211	230	0.288	285	0.356	**23.75**
V26	184	0.193	177	0.221	340	0.425	**92.03**
I30	180	0.189	190	0.237	244	0.305	**28.90**
D32	165	0.174	201	0.252	293	0.366	**45.46**
K33	125	0.132	123	0.154	138	0.173	**12.16**
I44	173	0.182	183	0.228	233	0.292	**27.73**
A46	126	0.133	160	0.200	175	0.219	**9.39**
E64	216	0.228	245	0.306	293	0.366	**19.59**
N60	208	0.219	193	0.242	277	0.346	**43.33**
average	165	0.174	178	0.222	242	0.302	36.26

Table S1A. Comparison of the H^N and Hα linewidth in FP and iFD ubiquitin. The linewidth improvement [%] was calculated as = [(LW[FP]/LW[iFD])-1]*100. See also table S1B for a complete list of resolved H^N and Hα protons in iFD ubiquitin.

	H^N 950 MHz [Hz]	H^N 950 MHz [ppm]
I3	149.83	0.16
K6	200	0.21
T7	141	0.15
T9	127	0.13
G10	134.65	0.14
K11	143.56	0.15
T12	81.54	0.09
I13	155.93	0.16
T14	102.35	0.11
L15	173.77	0.18
V17	140.53	0.15
S20	141.06	0.15
D21	119.04	0.13
T22	212.33	0.22
V26	193.87	0.20
K27	183.87	0.19
K29	179	0.19
K33	137.44	0.14
E34	164.95	0.17
I36	191.33	0.20
D39	202.26	0.21
Q40	173.33	0.18
Q41	143.7	0.15
R42	169.38	0.18
L43	225.42	0.24
I44	234.72	0.25
F45	155.05	0.16
A46	177.91	0.19
G47	118.76	0.13
K48	104	0.11
Q49	182	0.19
E51	216.4	0.23
D52	123.74	0.13
R54	122.9	0.13
T55	180	0.19
S57	320	0.34
Y59	119	0.13
I61	170.59	0.18
S65	86.72	0.09
T66	155.87	0.16
L69	190	0.20
average	162.0682927	0.17

	Hα 950 MHz [Hz]	Hα 950 MHz [ppm]
Q2	150.00	0.16
I3	188.00	0.20
F4	126.14	0.13
K6	226.00	0.24
L15	135.14	0.14
V17	102.51	0.11
E18	177.30	0.19
P19	200.07	0.21
S20	147.06	0.15
V26	183.63	0.19
I30	179.87	0.19
D32	165.41	0.17
K33	125.03	0.13
I36	138.41	0.15
I44	173.10	0.18
F45	260.00	0.27
A46	126.14	0.13
G47 α1	148.00	0.16
G47 α2	154.00	0.16
K48	264.97	0.28
K63	201.15	0.21
E64	216.23	0.23
Y59	88.68	0.09
N60	208.46	0.22
S65	130.99	0.14
average	168.65	0.18

Table S1B. Full list of resolved H^N and Hα signals in iFD ubiquitin at 950 MHz and 60 kHz MAS. Signals were analyzed without application of a window function in the ^{1}H-dimension.

S2. I. Quantitative analysis of the ^{1}H pattern in iFD ubiquitin using solution NMR

	Hα	Hβ	Hγ	Hγ2	Hδ	Hδ2	Hε
Ala	95	48					
Arg	96	97	/		87		
Asp	103	78					
Asn	93	74					
Cys	*						
Gln	88	93	50				
Glu	94	102	58				
Gly	95						
His	/	89					
Ile	95	99	77	57		70	
Leu	91	98	98		50	53	
Lys	89	79	72		97		94
Met	99	/	72				
Phe	102	70					
Pro	91	95			76		
Ser	93	24					
Thr	99	88	76				
Trp	*						
Tyr	97	65					
Val	96	99	55	44			

Table S2. Protonation levels [%] of aliphatic carbons were analyzed using ^{13}C-^{1}H HSQC[1] solution-state NMR spectra, measured at 900 MHz. The spectra were normalized (to account for different sample concentrations) following the procedure outlined in Ref. ([2]) by using ^{15}N-^{1}H HSQC spectra. All analysis was based on ^{1}H, ^{13}C and ^{15}N solution NMR assignments from Ref. ([3]). Note that this is exactly the same procedure that was successfully applied to analyze the protonation pattern in fractional deuterated (FD) ubiquitin.[4]

* = not present in ubiquitin

/ = not accessible due to spectral overlap

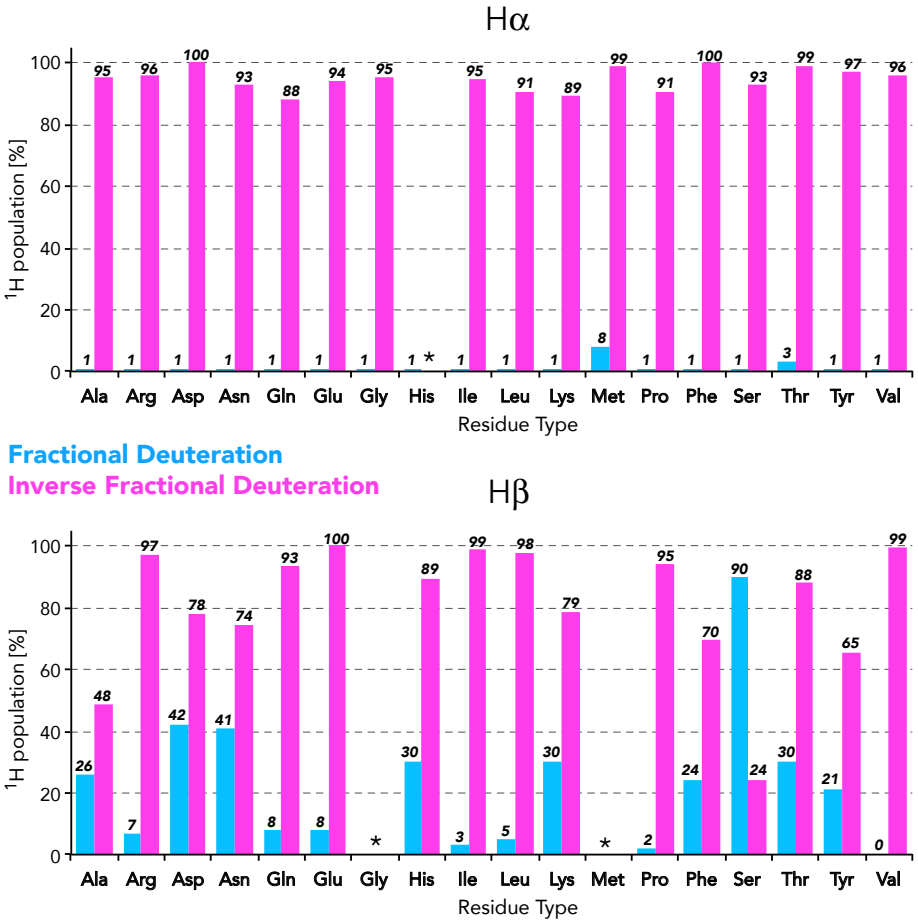

Figure S2A. Protonation levels for Hα and Hβ protons in iFD ubiquitin. The very high protonation levels a the Hα positions can be easily rationalized given that Hα are incorporated during protein expression from the solvent, which is proton-based (100 % H_2O) with iFD labelling, while the Hα levels are close to zero with D_2O-based FD labelling. The Hβ levels also correlate inversely with FD labelling.

S2. II. Discussion of the ^{1}H linewidth improvement in iFD ubiquitin

The linewidth improvement in iFD ubiquitin is not uniform because the reduction of the sidechain ^{1}H-levels is also not uniform (Table S2). For example, the resolution of GlyH^N does barely improve with iFD labelling, because Gly has no sidechain and the ^{1}H-density around GlyH^N hence hardly changes. The resolution of residues such as Ser, Phe, or Tyr improves substantially, because the Hβ-level is much reduced for these residue types. In general, what matters for the linewidth improvement is the reduction of the ^{1}H-density around a given ^{1}H, which depends on the 3D structure of a given protein (Figure S2B).

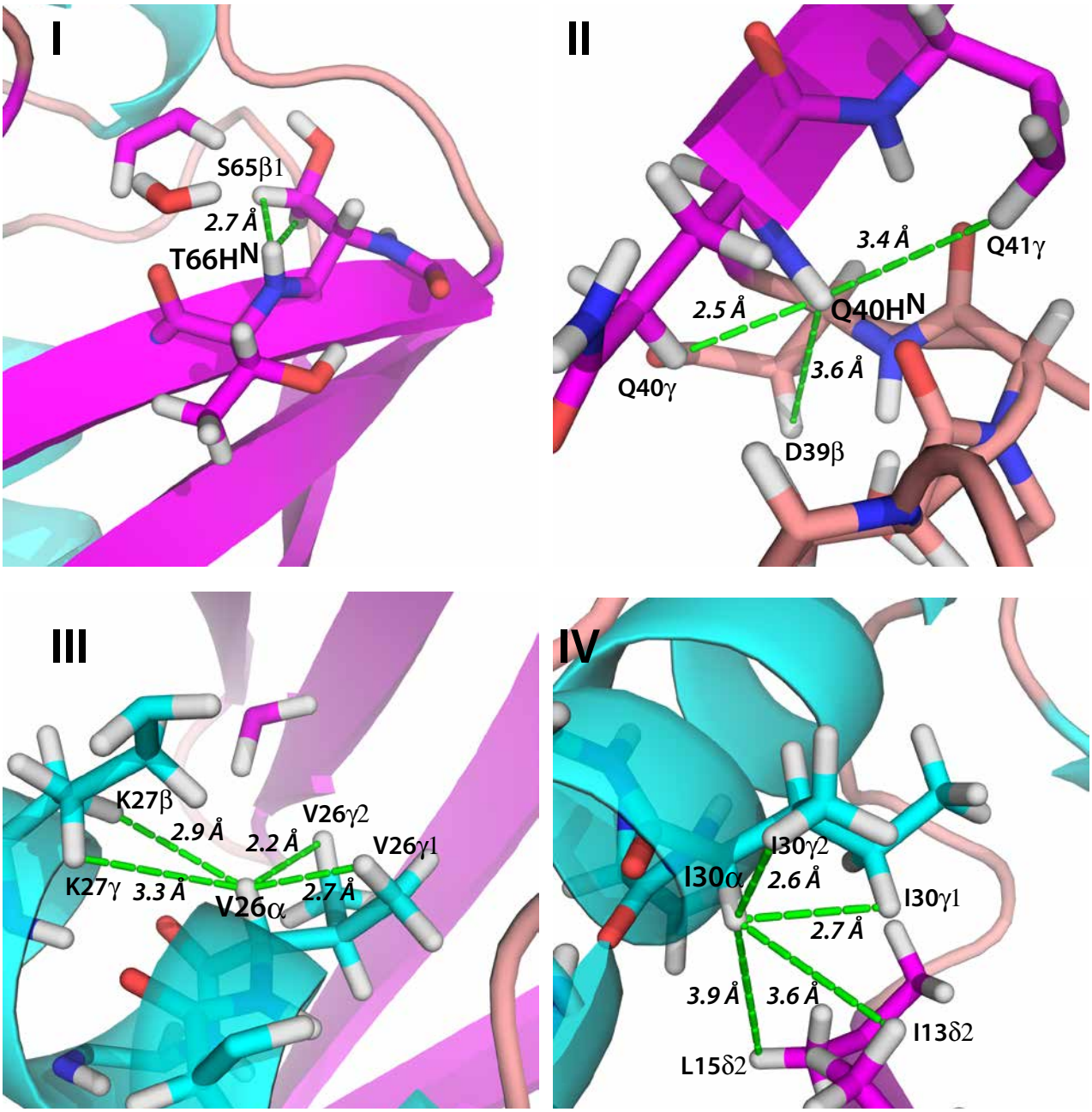

Figure S2B. Panels I-IV show examples of H^N and Hα which show relatively stark linewidth gains in iFD ubiquitin because the ^{1}H density in proximity is much reduced with iFD labelling (25 – 75 %).

Panel I (T66H^N): S65Hβ is the closest proton to T66H^N and has only ~25% ^{1}H-level with iFD labeling.
Panel II (Q40H^N): Three close-by sidechain ^{1}H (Q40γ/Q41γ/D39β) are only populated to ~50 %.
Panel III (V26α): Four near-by sidechain ^{1}H (K27β/K27γ/ V26γ1/V26γ2) are only populated to ~50-75 %.
Panel IV (I30α): Four close-by sidechain ^{1}H (I13δ2/L15δ2/ I30γ1/ I30γ2) are only populated to ~50-75 %.

S2. III. 2D comparison of iFD and FP ubiquitin

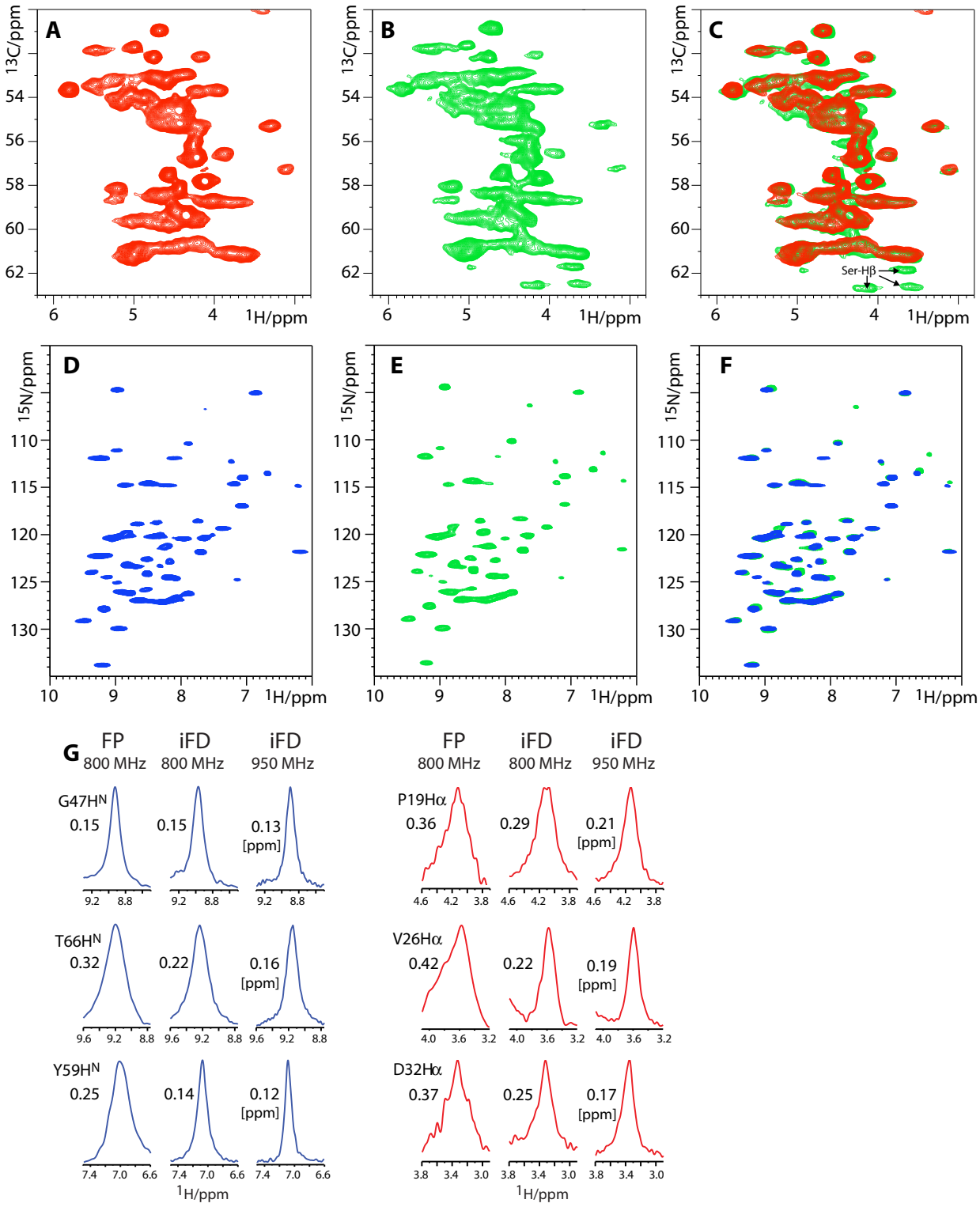

Figure S2C. 2D comparison of 2D CH (A,B) and NH (D,E) spectra measured with iFD (A,D) and FP (B,E) ubiquitin at 800 MHz and 60 kHz MAS. Overlays are shown in C and F. Processing parameters are the same for both sample preparations. For the Hα protons, it is readily visible that the ^{1}H-resolution is improved in iFD ubiquitin. A 2D comparison is less useful for the H^N, because they are well-resolved in both sample preparations. G) In 1D cross-sections (see also Figure 1C of the main text), it is however clearly discernible that the resolution is improved in iFD ubiquitin for both H^N and Hα. Note that the Hα are better resolved because they are closer to the ^{1}H-diluted side-chains.

S2. IV. Discussion of the sample quality

To fairly compare the ^{1}H-linewidth in FP and iFD ubiquitin, it is essential that the analysis is not biased by sample quality. We can deduce the sample quality from the ^{15}N-linewidth, which is most sensitive to sample heterogeneity. Our analysis showed virtually exactly the same ^{15}N linewidth for the compared ubiquitin samples, also for residues such as D21, Y59, and S65 (Figure S2D), which show large gains in ^{1}H-resolution in iFD ubiquitin. This clearly demonstrates that the ^{1}H-resolution improvement is caused by the reduction in the ^{1}H-density.

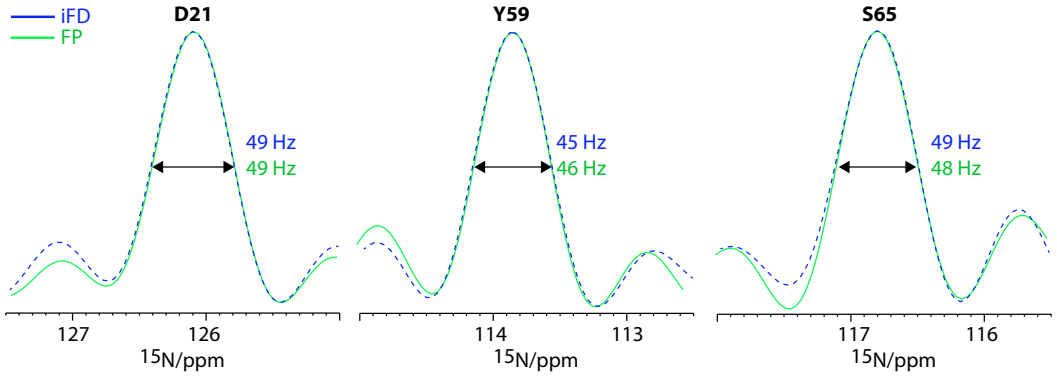

Figure S2D. Overlay of ^{15}N cross-sections of FP (green) and iFD (blue) ubiquitin.

S3. Linewidth of side chain protons

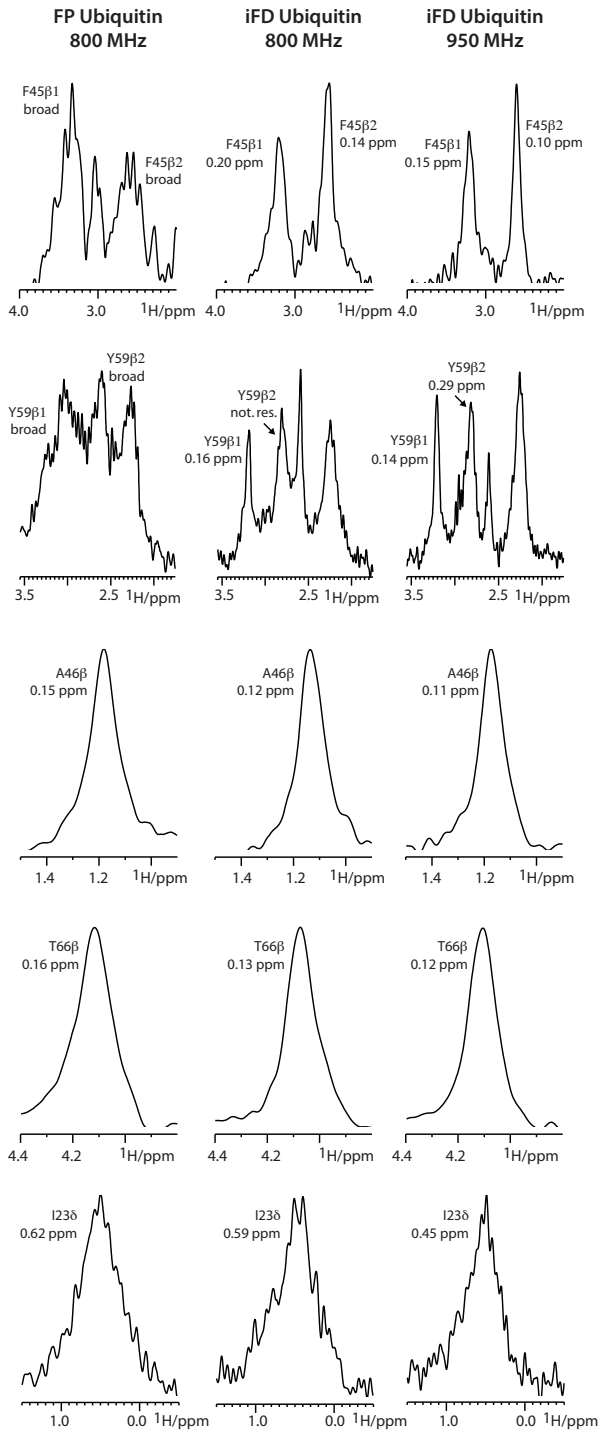

Figure S3. t_1 cross-sections, extracted from 2D CH experiments measured at 60 kHz MAS, showing the linewidth of side chain ^{1}H. We generally found an improved ^{1}H linewidth in iFD ubiquitin compared to FP ubiquitin, which is very pronounced for certain residue types such as Phe and Tyr. The improvement was marginal for certain methyl-groups (see e.g. I23δ) due isotopologue effects.

S4. Spectral overlay of water-accessible and -inaccessible residues

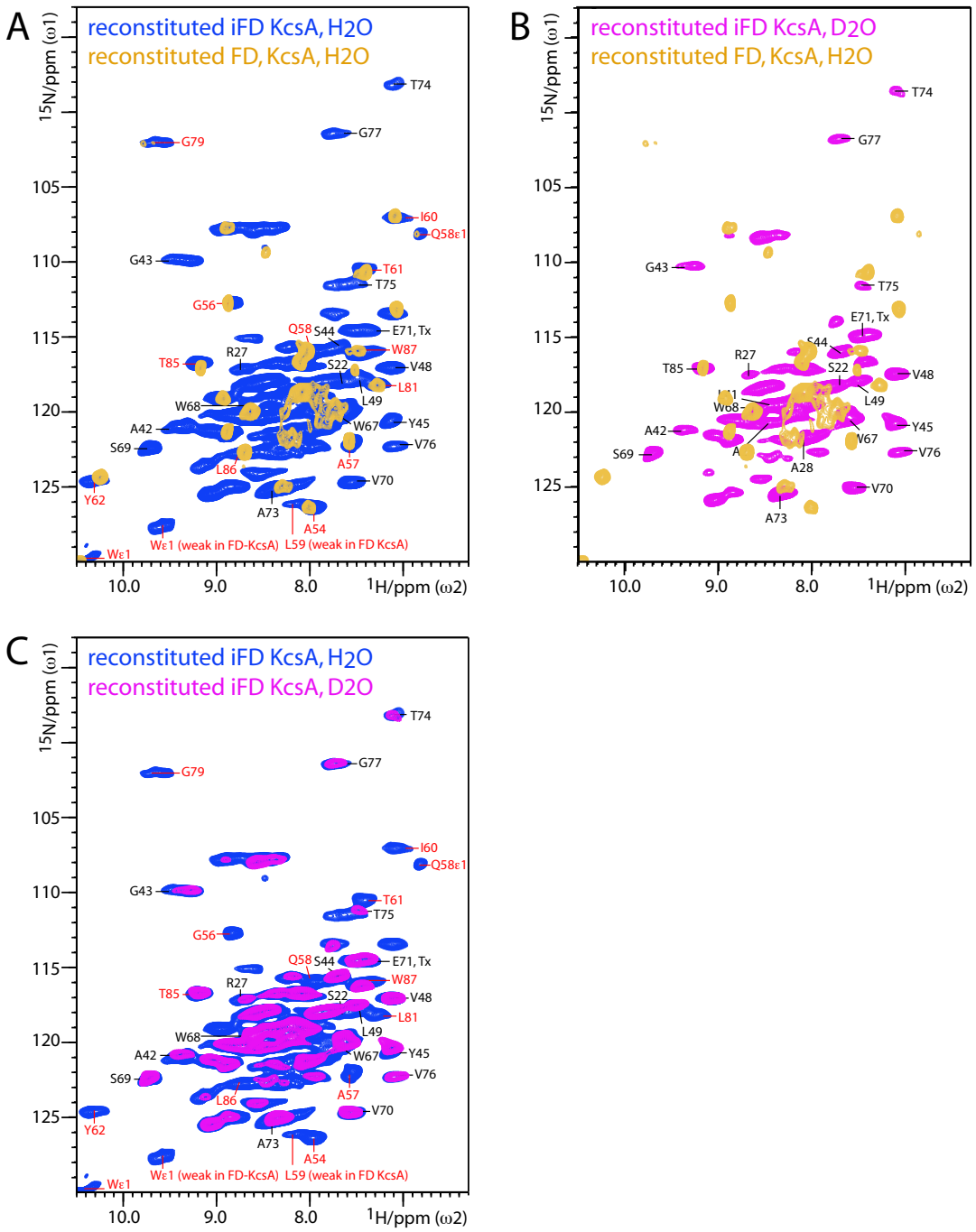

Figure S4. Spectral overlay of 2D NH spectra measured with A) iFD KcsA in H_2O (blue signals) and FD[4] KcsA in H_2O (yellow signals). iFD KcsA (in H_2O), which was expressed in protonated solvents, features all H^N signals, while FD KcsA (in H_2O), which was expressed in deuterated solvents, shows only water-accessible residues. Red annotations correspond to signals that were previously assigned in FD KcsA, black signals were assigned with iFD KcsA. B) Overlay of FD KcsA and D_2O-washed iFD KcsA. It can be readily seen that all signals of the turret (with exception of T85) as well as G79 of the upper part of the selectivity filter disappear in the iFD KcsA spectrum after D_2O-wash. Therefore, the combination of iFD and FD labelling is also an attractive tool to study membrane protein topology. C) Overlay of iFD KcsA before (in blue) and after D_2O-wash (in magenta). It is readily visible that the spectral resolution is improved in the magenta spectrum.

S5. ^{1}H-linewidth comparison in iFD KcsA before and after incubation in D_2O

	in vitro	in vitro	in vitro	in vitro	in vitro	in situ	in situ
	iFD (D_2O)	iFD (D_2O)	iFD (H_2O)	iFD (H_2O)		iFD (D_2O)	iFD (D_2O)
Residue	**LW [Hz]**	**[ppm]**	**LW [Hz]**	**[ppm]**	**Improv. [%]**	**LW [Hz]**	**[ppm]**
G43	350	0.44	358	0.45	2.29	249	0.31
S44	194	0.24	overlap	overlap		overlap	overlap
V48	160	0.20	204	0.26	27.50	198	0.25
W68	160	0.20	overlap	overlap		overlap	overlap
S69	107	0.13	135	0.17	26.17	210	0.26
V70	162	0.20	204	0.26	25.89	209	0.26
A73	163	0.20	265	0.33	62.36	321	0.40
T74	227	0.28	238	0.30	4.85	190	0.24
V76	227	0.28	300	0.38	32.16	280	0.35
T75	178	0.22	384	0.48	115.73	416	0.52
G77	244	0.31	288	0.36	18.03	416	0.52
T85	142	0.18	210	0.26	47.89	176	0.22
X1	187	0.23	232	0.29	0.24	151	0.19
X2	169	0.21	overlap	overlap	overlap	overlap	overlap
X3	224	0.28	~400	~0.50	~75	gone	gone
X4	153	0.19	~340	~0.42	~120	overlap	overlap

Table S5. Linewidth of H^N resonances that were well resolved in the in vitro KcsA (D_2O) 2D NH spectrum. The linewidth improvement [%] was calculated as = [(iFD [H_2O]/iFD [D_2O])-1]*100. See Figure S5 below for signals X1-X4.

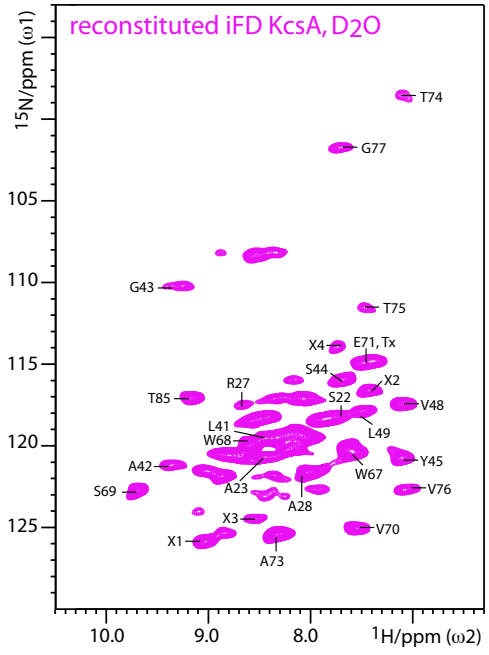

Figure S5. 2D NH spectrum of D_2O-washed iFD KcsA. The unassigned signals X1 – X4, which were included in the linewidth analysis, are indicated in the spectrum.

S6. Spectral overlay of D_2O-washed iFD KcsA in reconstituted bilayers and in native bacterial cell membranes

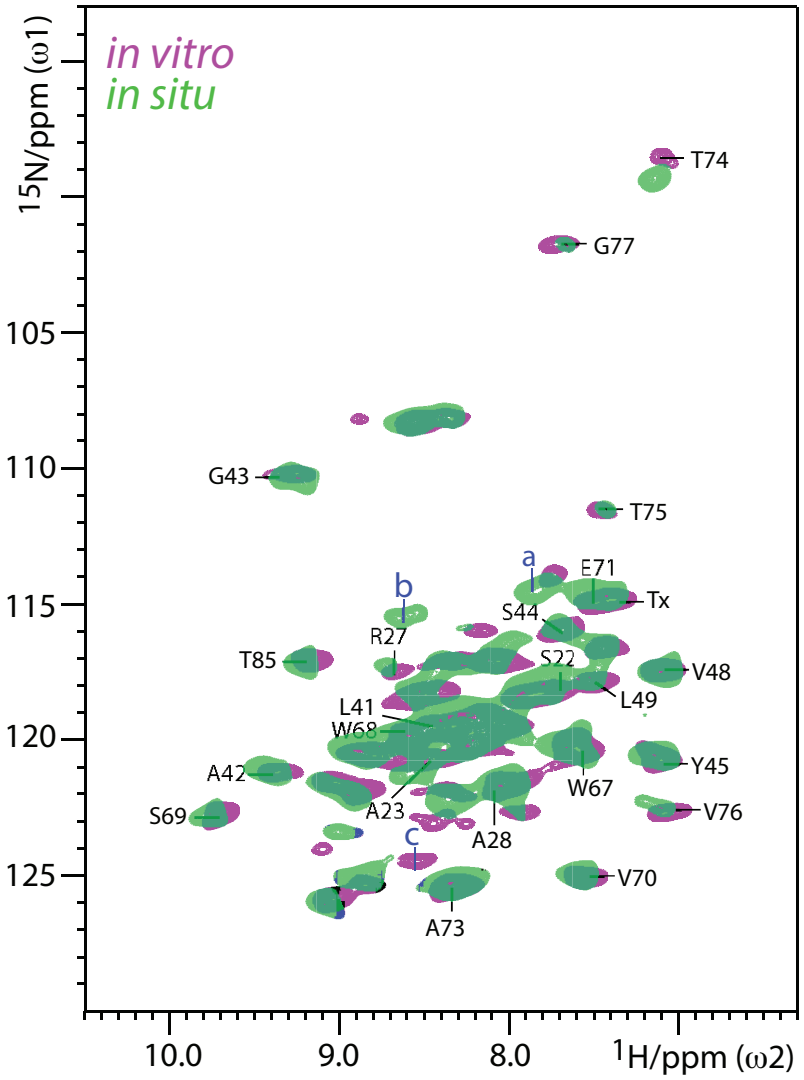

Figure S6. Spectral overlay of Figures 2B and 2E of the main text, i.e., of *in vitro* (in magenta) and *in situ* (in green) D_2O-washed iFD KcsA. The spectra superimpose very well, with exceptions being T74 (see Figure 3 of the main text), as well as the unassigned signals a, b and c. Signal a is a Threonine residue and shows a large CSP (+0.6 ^{15}N ppm). Signal b is present in *in vitro* KcsA, however much weaker than in native cell membranes, which suggests local topology differences between the two samples. Differences in the topology and water-accessibility are presumably also the reasons for the absence of signals c in *cellular* KcsA, since signal c became also weaker in the reconstituted KcsA sample over time.

S7. ^{1}H-linewidth comparison *in vitro* / *in situ* D_2O-incubated iFD KcsA

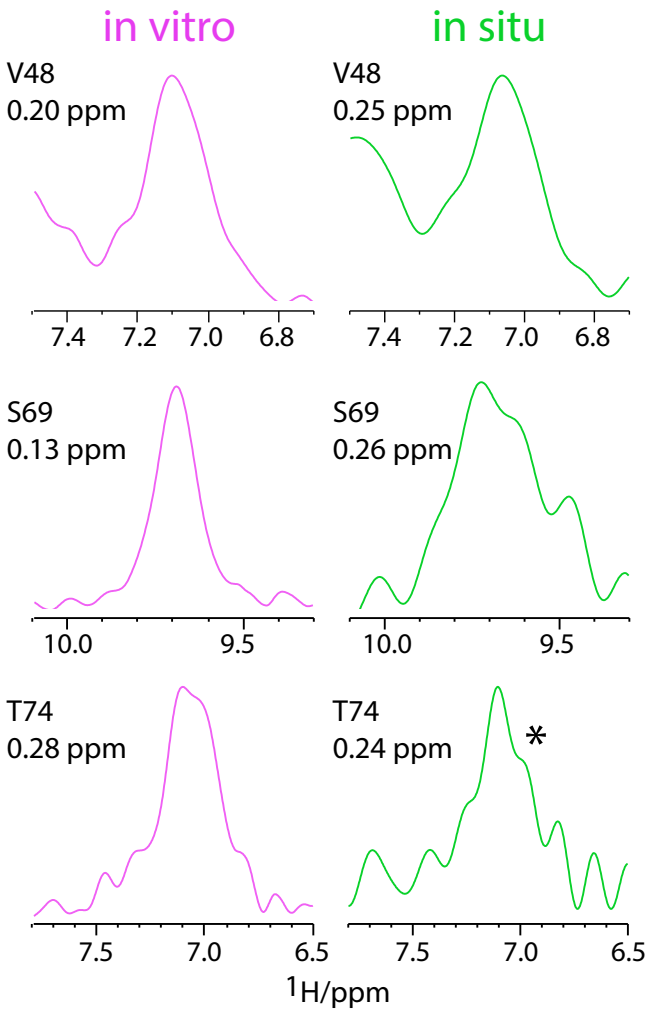

Figure S7. t_1 cross-sections, extracted from the 2D NH spectra shown in Figure 2B and 2E of the main text. See also Table S5.

* S/N ratio of T74 in cellular KcsA was ~7.3 and potentially too low for a correct determination of the linewidth.

S8. G104 and G116 of the TM2 helices are likely exchanged in D_2O-inacubated KcsA.

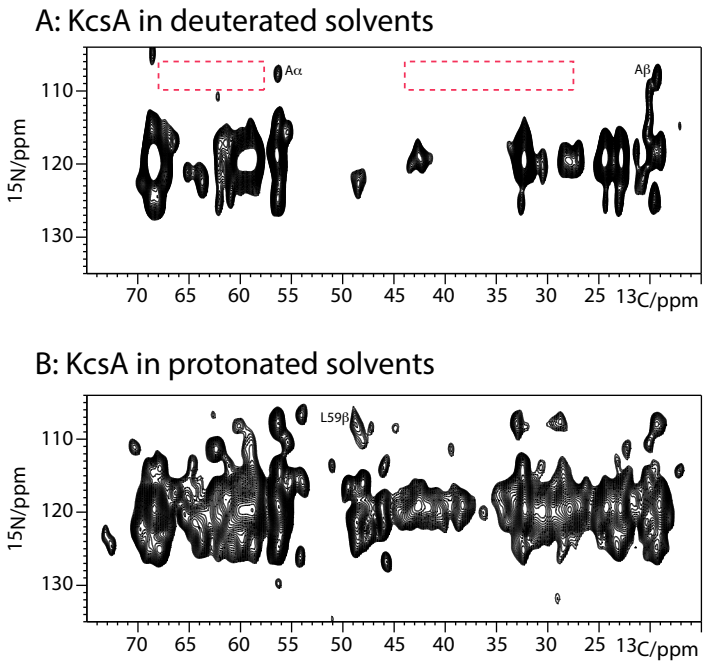

Figure S8. Cut-out from a 2D N(CO)CX spectra of A) D_2O-incubated FP KcsA, measured at 800 MHz and 17 kHz MAS and B) H_2O-incubated KcsA measured at 700 MHz and 14 kHz MAS. In A), the ^{1}H-^{15}N CP contact time was keep very short (250 µs) to select water-inaccessible residues with protonated H^N, as described in Ref ([5]). We obtained a very good selection of the water-inaccessible residues, as judged by the complete absence of water-accessible residues of the turret loop in a NCα spectrum with 250 µs ^{1}H-^{15}N CP contact time (not shown).

In Figure 2B of the main text, only two glycine residues (at 107-108.5 ^{15}N ppm / 8.3 – 8.7 ^{1}H ppm) are not assigned. While we cannot be sure how many glycines we observe in the 2D N(CO)CX spectrum A) around 107-108.5 ^{15}N ppm, we do not observe the flexible hinge G104[6,7] and G116 in spectrum A), because the preceding residues F103 and V115, respectively, cannot be detected (they should show Cα signals around 60-65 ppm and potentially Cβ around ~45-25 ppm (red empty boxes)). We only observe alanine residues (which can stem from G43->A42, G30->A29 and G99->A98) in spectrum A). Hence, G104 and G116 residues have presumably (partly) exchanged in D_2O. They may potentially also show dynamics which interfere which the SPECIFIC CP transfer.

S9. Measurement of the bulk ^{15}N $T_{1\rho}$ as a function of the ^{15}N spinlock power

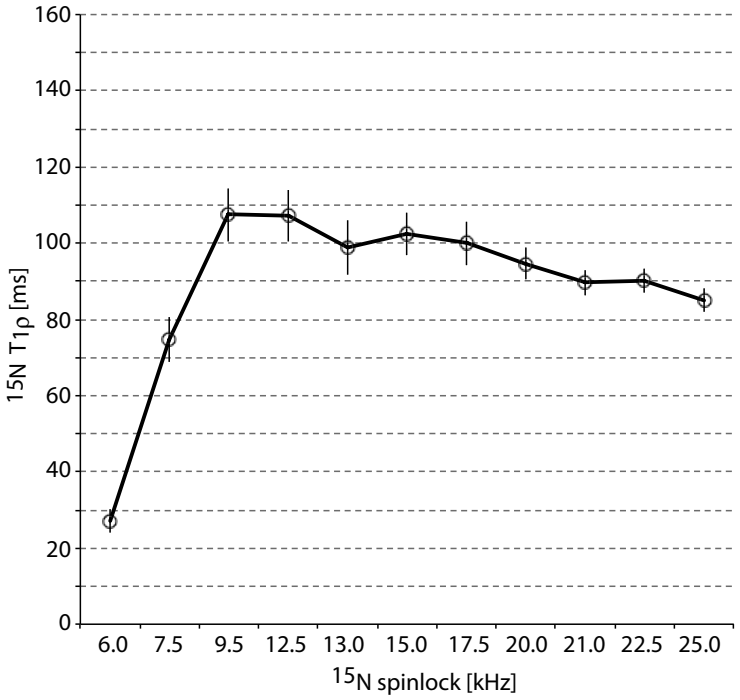

Figure S9. Bulk ^{15}N $T_{1\rho}$ measured in D_2O-washed iFD KcsA at 800 MHz and 60 kHz MAS. In line with Refs. ([8-10]), the graph shows a plateau from ~10 – 25 kHz ^{15}N spinlock power with an average ^{15}N $T_{1\rho}$ of ~100 ms. The relaxation time gets shorter with higher spinlock powers, presumably due to the proximity to the n=1/2 rotary resonance condition.

S10. Qualitative concentration determination of KcsA in the native inner cell membrane

We can qualitatively derive the concentration by comparing the signal to noise (S/N) ratios of the 2D NH spectra measured *in situ* and *in vitro* (Figures 2B and 2E of the main text, respectively).

For the comparison of the S/N, we used the well-resolved peaks listed in Figure 3G of the main text. We used peak heights and not integrals for the S/N comparison. Therefore we did not consider signals S69, A73, T75, and G77 for the S/N analysis, because these signals are substantially broader *in situ* than *in vitro*. Likewise, T85 was not used because its signal intensity is attenuated over time by H/D exchange with the deuterated solvent. We however considered one well-resolved, unassigned signal (signal X1 in Figure S5) to improve statistics.

S/N comparison

	vitro	situ	vitro/situ
G43	16.34	9.81	1.66
S44	28.62	14.10	2.03
Y45	30.50	14.47	2.11
V48	35.12	13.95	2.52
V70	32.50	10.62	3.06
T74	10.99	7.33	1.50
V76	18.16	5.30	3.43
X1	28.75	10.77	2.67
			2.37 **average**

Hence, by a conservative estimate, the S/N *in vitro* is twice higher than *in situ*. Since the 2D NH *in situ* was measured with 13.2*times the numbers of scans (NS) as compared with *in vitro*, we can qualitatively derive that the KcsA concentration *in vitro* is ~7 times higher than in the native cell membrane:

$$\frac{KcsA.conc_{vitro}}{KcsA.conc_{situ}} = \sqrt{13.2} * 2.0 \approx 7.2$$

(Note that the S/N increases with the square root of NS, hence the factor $\sqrt{13.2}$)
Since we know how much *in vitro* KcsA we filled in a 1.3 mm rotor, we can now derive the KcsA concentration *in situ*:

MW KcsA (^{13}C,^{15}N labeled) ≈ 78400 g/mol
Sample in rotor ≈ 2.5 mg
KcsA was reconstituted at 1/100 protein: lipid ratio, roughly corresponding to a 1/1 w/w ratio.
In a 1.3 mm rotor, we have hence ~1.25 mg of KcsA (~ 16 nanomoles).

In situ, we have hence only ~175 µg of KcsA in the rotor, corresponding to ~2.5 nanomoles. This explains why we needed almost 10.000 scans (see *Experimental Details* below) to acquire a sensitive 2D NH of KcsA in the inner membrane.

Figure S11. Chemical shift perturbations in *cellular* KcsA as compared to *in vitro* KcsA

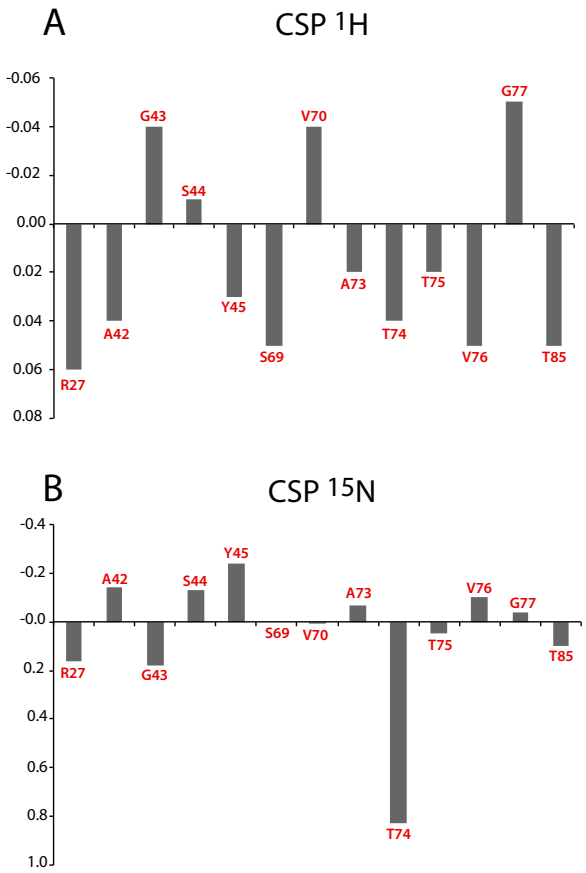

Figure S11. Chemical shift perturbations (CSP) of assigned and resolved peaks derived as the chemical shift difference between signals in 2D NH spectra of *in situ* and *in vitro* D_2O-washed iFD KcsA (i.e., CSP = *in situ* – *in vitro*). The CSPs are relatively small, especially for the protons.

Experimental details

^{1}H-detected

All 3D ssNMR experiments were measured at 800 MHz and 60 kHz MAS. The effective sample temperature was set to ~308 K. Water suppression was achieved with the MISSISSIPPI scheme[11]. Decoupling was performed with the PISSARRO scheme[12,13] during all direct and indirect acquisition periods. For all experiments and all nuclei, the decoupling amplitude was set to one quarter of the MAS frequency, i.e., 15 kHz and not further optimised. Decoupling times were optimized between 50 and 74 µs for all nuclei. For all experiments, quadrature-detection in the indirect dimensions was achieved using TPPI. The pulse sequence used to acquire 2D ^{13}C/^{15}N - ^{1}H spectra was described in Ref. ([14]). The recycle delay ('d1 time') was ~0.8 – 1.0s for all ^{1}H-detected measurements. For all 2D spectra / planes shown in the manuscript and the Supporting Information, we used a contour level increment of 1.05 – 1.10 and 50 – 60 contour levels. For all measurements, we used sparse Poisson-Gap[15] sampling (see below for details) and reconstruction was done with compressed sensing[16] in Topspin 3.2 (Bruker Biospin). Note that all 3D experiments performed on KcsA were done with the D_2O-incubated *in vitro* sample. Pulse sequence diagrams for the herein used experiments were already been published elsewhere.[4]

3D CαNH

The initial ^{1}H -> ^{13}C transfer was brought about with ramped (20 %) cross polarization with contact times of 450 µs and 500 µs for iFD ubiquitin and iFD KcsA (D_2O), respectively. Polarization was transferred further from ^{13}Cα -> ^{15}N with SPECIFIC CP[17] using 41 kHz irradiation on ^{13}C and 20 kHz on ^{15}N during 6.0 ms for both iFD ubiquitin and iFD KcsA (D_2O). Despite the relatively strong irradiation on the ^{13}C channel, the transfer was specific for Cα, which was achieved by moving the ^{13}C carrier upfield (to ~0 ppm), away from the CO signal region. No decoupling on ^{1}H was necessary during SPECIFIC CP transfer, since heteronuclear dipolar couplings involving ^{1}H are much reduced at 60 kHz MAS in iFD proteins. The final transfer from ^{15}N -> ^{1}H was carried out with ramped (10 %) cross-polarization (65 kHz on ^{15}N, 124 kHz on ^{1}H, 750 µs contact time for iFD ubiquitin, 500 µs for iFD KcsA). The measurement time was 14h for ubiquitin and 2d 20h for KcsA using sparse [66 % for ubiquitin / 50 % for KcsA] sampling.

3D CONH

Analogous to the CαNH experiment. The ^{1}H -> ^{13}C CP contact time was 3 ms in iFD KcsA (D_2O). SPECIFIC CP from CO to ^{15}N was established with 41 kHz irradiation on ^{13}C and 20 kHz irradiation on ^{15}N during 6.0 ms in the absence of ^{1}H decoupling. The ^{13}C carrier was placed at ~165 ppm during the SPECIFIC CP step. ^{15}N -> ^{1}H CP was carried out as described in the CαNH experiment. The measurement time was 2d 11h for KcsA using sparse [54 %] sampling.

3D NCαHα

After ^{1}H -> ^{15}N ramped (20 %) CP transfer over 1.5 ms (125 kHz on ^{1}H, 50 kHz on ^{15}N), ^{15}N -> ^{13}Cα transfer was performed with SPECIFIC CP over 6.0 ms, during which the ^{13}C carrier was placed ~0 ppm (as described above). The final transfer from ^{13}Cα -> ^{1}H was done with ramped (10 %) cross-polarization using 185 µs contact time. The measurement time was 2d 12h for iFD ubiquitin using sparse [70 %] sampling.

3D Cα(CO)NH

^{1}H -> ^{13}C CP transfer was performed with 500 µs contact time and the ^{13}C carrier placed at ~-10 ppm, which yielded selective transfer to the aliphatic carbons, as described in Refs. ([4,18]). ^{13}C-^{13}C mixing was brought about with double quantum DREAM[19] recoupling using 27 kHz recoupling amplitude (20 % ramp) over 6.25 ms. Best transfer performance was achieved with the ^{13}C carrier close to the ^{13}CO region (~170 ppm) during the transfer. No ^{1}H-decoupling was applied during DREAM recoupling, which did not lead to any perceivable transfer losses in comparison to the application of ^{1}H-decoupling. The following ^{13}CO –> ^{15}N –> ^{1}H transfer steps were analogous to the ones described in the 3D CONH experiment. The measurement time was 8d 8h for iFD KcsA (D_2O) using sparse [46 %] sampling.

3D CO(Cα)NH

Analogous to the CO(Cα)NH experiment. The ^{13}C carrier was placed at ~ 185 ppm during the initial ^{1}H -> ^{13}C CP step, which yielded selective transfer to the carbonyl carbons. ^{13}C-^{13}C mixing was brought about with double quantum DREAM[19] recoupling using 27 kHz recoupling amplitude (20 % ramp) over 4.3 ms. Best transfer performance was achieved with the ^{13}C carrier close to the ^{13}Cα region (~65 ppm) during the transfer. The following ^{13}Cα –> ^{15}N –> ^{1}H transfer steps were analogous to those described in the 3D CαNH experiment. The measurement time was 6d 18h for iFD KcsA (D_2O) using sparse [50 %] sampling.

3D CCH

^{1}H -> ^{13}C CP transfer was performed with 450 µs contact time in iFD ubiquitin. ^{13}C-^{13}C mixing was brought about with double quantum DREAM[19] recoupling using 27 kHz recoupling amplitude (20 % ramp) over 3.5 ms with the ^{13}C carrier placed at ~55 ppm.

^{13}C -> ^{1}H transfer was done with a short (200 µs) CP step to ensure one-bond transfer. The measurement time was 3d 2h in iFD ubiquitin using sparse [60 %] sampling.

2D NH in *cellular* KcsA

This experiment was performed with 9760 scans (i.e., 13.2*times more scans than for the corresponding experiment with KcsA *in vitro*) and had a total duration of 5d 16h.

^{13}C-detected

All ^{13}C-detected experiments were carried out with FP KcsA.

3D NCαCX

This experiment was carried out at 500 MHz and 12 kHz MAS and a real temperature of ~278 K. The initial ^{1}H -> ^{15}N transfer time was keep very short (250 µs) to select only water-inaccessible residues with protonated backbone nitrogens. The selection was very good, which was verified in a 2D NCα experiment, in which all residues of the water-accessible turret loop were absent. The measurement time was 9d 15h using sparse [72 %] sampling.

2D N(CO)CX

This experiment was carried out at 800 MHz and 17 kHz MAS and a real temperature of ~278 K. Analogously to the 3D NCαCX experiment, the initial ^{1}H -> ^{15}N transfer time was keep very short (250 µs) to select only water-inaccessible residues with protonated backbone nitrogens. The measurement time was 2d 15h using conventional sampling.

^{15}N $T_{1\rho}$ measurements

^{1}H-detected ^{15}N $T_{1\rho}$ measurements were carried out as described in Refs. ([8,10]) with the below shown pulse sequence (Figure S12). All measurement were performed at 800 MHz magnetic field with 60 kHz MAS using recycle delays of 0.9 s. The ^{15}N transverse magnetization decay was probed with a ^{15}N spinlock field of 20 kHz. No ^{1}H-decoupling was applied during the ^{15}N spinlock. Note that we found a ^{15}N $T_{1\rho}$ plateau from ~10–25 kHz spinlock power (Figure S9). Five points with 0, 20, 50, 100, and 200 ms duration of the spinlock were taken. The signals were processed with QSIN 3 window functions in both ^{1}H and ^{15}N dimensions to enhance the resolution. Only well-isolated peaks were considered for the analysis, for which we measured the peak intensities. The $T_{1\rho}$ trajectories were fit to single exponentials. Note that for G43, which shows a signal splitting (Figure 3 C,D of the main text), we used the maximal intensity of both conformations, given it was not possible to resolve the two conformations in the absence of a relaxation filter.

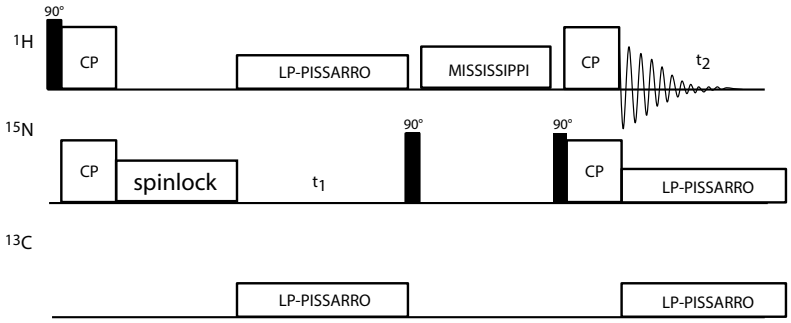

Figure S12. NMR pulse sequence to measure site-resolved ^{15}N $T_{1\rho}$ in the TM part of KcsA.

Sample Preparation

iFD ubiquitin

Inverse Fractional Deuterated ubiquitin - The protein was expressed in *E.coli* BL21 cells on H_2O-based M9 medium supplemented with 0.5 g/L $^{15}NH_4Cl$ and 2 g/L D-glucose-$^{13}C_6$-d7. The purification procedure and further sample preparation was followed as described previously.[14] Obtained yield was ~16 mg/L. *Fully Protonated ubiquitin* - FP ubiquitin followed the same procedure, except that fully protonated D-glucose-$^{13}C_6$ was supplemented instead of deuterated glucose. The yield was ~20 mg/L.

iFD KcsA

in vitro Inverse Fractional Deuterated KcsA - KcsA was expressed in *E.coli* M15 cells using standard H_2O-based M9 medium supplemented with 0.5 g/L $^{15}NH_4Cl$ and 2 g/L D-glucose-$^{13}C_6$-d7. The protein was extracted and purified as described previously,[20] resulting in a final yield of 10 mg/L. Liposome reconstitution was performed using *E.coli* polar lipids (Avanti) at 1:100 protein:lipid molar ratio using polystyrene beads (Bio-Beads SM-2), as also previously described.[20] Before the ssNMR measurements, reconstituted samples were suspended in fully protonated phosphate buffer or, for D_2O-washed KcsA, twice washed in fully deuterated phosphate buffer (50mM pH7, 50mM NaCl and KCl). The D_2O-washed sample was twice incubated in ~1 ml of deuterated buffer for a total of three days prior to the measurements.

in situ Inverse Fractional Deuterated KcsA - KcsA was expressed in *E.coli* Lemo21 cells using the T7 inhibition system as described in Ref. ([21]). Cells were first grown in unlabeled M9 media until saturation. Prior to induction, the cells were harvested and re-suspended in an H_2O-based M9 medium supplemented with 0.1 mg/mL rifampicin, 0.5 g/L $^{15}NH_4Cl$ and 2 g/L D-glucose-$^{13}C_6$-d7. After expression, cells were washed, lysed and the cellular membranes were extracted. The different membrane fractions were separated according to their density difference using a sucrose gradient (gradient (w/v) 36%, 45%, 51%, 55 %). The inner membrane fraction was collected, twice washed and incubated in ~1ml of deuterated phosphate buffer (pH7) for a total of three days before the ssNMR measurements. This procedure (except for the D_2O-wash) is described with greater detail in Ref. ([21]).

References

(1) Bodenhausen, G.; Ruben, D. J. *Chem Phys Lett* **1980**, *69*, 185.
(2) Otten, R.; Chu, B.; Krewulak, K. D.; Vogel, H. J.; Mulder, F. A. *Journal of the American Chemical Society* **2010**, *132*, 2952.
(3) Cornilescu, G.; Marquardt, J. L.; Ottiger, M.; Bax, A. *Journal of the American Chemical Society* **1998**, *120*, 6836.
(4) Mance, D.; Sinnige, T.; Kaplan, M.; Narasimhan, S.; Daniels, M.; Houben, K.; Baldus, M.; Weingarth, M. *Angew Chem Int Ed Engl* **2015**, *54*, 15799.
(5) Shi, L. C.; Kawamura, I.; Jung, K. H.; Brown, L. S.; Ladizhansky, V. *Angew Chem Int Edit* **2011**, *50*, 1302.
(6) Cuello, L. G.; Jogini, V.; Cortes, D. M.; Perozo, E. *Nature* **2010**, *466*, 203.
(7) Cuello, L. G.; Jogini, V.; Cortes, D. M.; Sompornpisut, A.; Purdy, M. D.; Wiener, M. C.; Perozo, E. *Febs Lett* **2010**, *584*, 1133.
(8) Lewandowski, J. R.; Sass, H. J.; Grzesiek, S.; Blackledge, M.; Emsley, L. *J Am Chem Soc* **2011**, *133*, 16762.
(9) Good, D. B.; Wang, S. L.; Ward, M. E.; Struppe, J.; Brown, L. S.; Lewandowski, J. R.; Ladizhansky, V. *Journal of the American Chemical Society* **2014**, *136*, 2833.
(10) Lamley, J. M.; Oster, C.; Stevens, R. A.; Lewandowski, J. R. *Angew Chem Int Ed Engl* **2015**, *54*, 15374.
(11) Zhou, D. H.; Rienstra, C. M. *J Magn Reson* **2008**, *192*, 167.
(12) Weingarth, M.; Bodenhausen, G.; Tekely, P. *Journal of Magnetic Resonance* **2009**, *199*, 238.
(13) Weingarth, M.; Tekely, P.; Bodenhausen, G. *Chem Phys Lett* **2008**, *466*, 247.
(14) Sinnige, T.; Daniels, M.; Baldus, M.; Weingarth, M. *Journal of the American Chemical Society* **2014**, *136*, 4452.
(15) Hyberts, S. G.; Takeuchi, K.; Wagner, G. *J Am Chem Soc* **2010**, *132*, 2145.
(16) Holland, D. J.; Bostock, M. J.; Gladden, L. F.; Nietlispach, D. *Angew Chem Int Edit* **2011**, *50*, 6548.
(17) Baldus, M.; Petkova, A. T.; Herzfeld, J.; Griffin, R. G. *Mol Phys* **1998**, *95*, 1197.
(18) Chevelkov, V.; Habenstein, B.; Loquet, A.; Giller, K.; Becker, S.; Lange, A. *J Magn Reson* **2014**, *242*, 180.
(19) Verel, R.; Baldus, M.; Ernst, M.; Meier, B. H. *Chem Phys Lett* **1998**, *287*, 421.
(20) van der Cruijsen, E. A.; Nand, D.; Weingarth, M.; Prokofyev, A.; Hornig, S.; Cukkemane, A. A.; Bonvin, A. M.; Becker, S.; Hulse, R. E.; Perozo, E.; Pongs, O.; Baldus, M. *Proc Natl Acad Sci U S A* **2013**, *110*, 13008.
(21) Baker, L. A.; Daniels, M.; van der Cruijsen, E. A. W.; Folkers, G. E.; Baldus, M. *Journal of Biomolecular Nmr* **2015**, *62*, 199.